UKAEA-RACE-CP(21)02

Emil T. Jonasson, Luis Ramos Pinto, Alberto Vale,
Robert Skilton

Comparison of three key remote sensing technologies for mobile robot localization in nuclear facilities

Comparison of three key remote sensing technologies for mobile robot localization in nuclear facilities

Emil T. Jonasson, Luis Ramos Pinto, Alberto Vale, Robert Skilton

This paper has been submitted to
31st Symposium on Fusion Technology (SOFT), Dubrovnik, Croatia, 20 - 25 September 2020

Comparison of three key remote sensing technologies for mobile robot localization in nuclear facilities

Emil T. Jonasson*[a], Luis Ramos Pinto[b], Alberto Vale[b]

[a]RACE, UKAEA, Culham Science Centre, Abingdon, United Kingdom
[b]Institute for Plasmas and Nuclear Fusion, University of Lisbon, Portugal

Abstract

Sensor technologies will play a key role in the success of Remote Maintenance (RM) systems for future fusion reactors. In this paper, three key types of sensor technologies of particular interest in the robotics field at the moment are evaluated, namely: Colour-Depth cameras, LIDAR (Light Detection And Ranging), and Millimetre-Wave (mmWave) RADAR. The evaluation of the sensors is performed based on the following criteria: the types of data they provide, the accuracy at different distances, and the potential environmental resistance of the sensor (namely gamma radiation). The authors review the progress in making these three types of sensor capable of operating in Fusion facilities and discuss possible mitigations. Experiments are performed to demonstrate the pros and cons of each type of sensor by collecting data from radar, colour-depth camera and LIDAR, simultaneously. The paper concludes with a performance comparison between sensors, as well as discussing the possibility of combining them, fostering redundancy in case of failure of any individual sensor device.

Keywords: Remote Sensing, Mobile robotics, Nuclear Maintenance, Radar, LIDAR, Depth Camera

1. Introduction

Sensor technologies will play a key role in the success of Remote Maintenance (RM) systems for future fusion reactors such as ITER (International Thermonuclear Experimental Reactor) and EU-DEMO (the European Union DEMOnstration fusion power reactor). Large parts of these facilities will be completely off-limits to human personnel due to the extremely high radiation levels in and around the reactor. This means that the vast majority of maintenance operations must be performed remotely. The facilities will be composed of 3 main types of areas where RM will be required: In-Vessel, Ex-Vessel and Active Maintenance Facilities. The operation of ex-vessel transportation is one of the key issues during maintenance, since the mobile platforms of transportation have to carry the activated material extracted from the reactor to a maintenance facility.

The nuclear environment has a set of unique challenges compared to more traditional industrial environments, which makes the use of mobile robotics with on-board sensing equipment especially challenging. The high radiation levels present will degrade the digital components of the sensors and any on-board processing devices. In addition, there are several other constraints in these scenarios such as residual magnetic fields (with a strong impact on electronic devices), cluttered conditions for operation, and levels of dust.

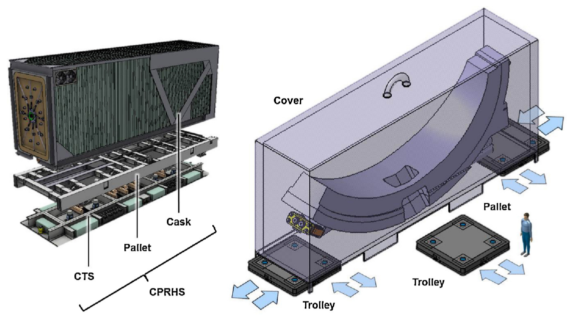

Figure 1: The cask and plug remote handling system of ITER (left image) and the design proposed for the ex-vessel transfer cask for DEMO (right image), [1]. This system handles ex-vessel transportation of, amongst other things, activated material extracted from the reactor.

However, these challenges must be overcome in order to ensure the successful maintenance of both ITER

*Corresponding author
Email address: `emil.jonasson@ukaea.uk` (Emil T. Jonasson*)

[2] and DEMO [1] [3] since the proposed RM solutions both currently rely on independent mobile Autonomous Ground Vehicles (AGVs) transferring equipment, tooling and components all around the reactor building and maintenance facilities (Figure 1). The sensors enabling this transportation work will need to be installed onboard the AGVs and are thus exposed to any radiation in the present environment as well as radiation coming from the transported load.

High reliability will be critical, since in case of sensor failure a recovery and rescue operation may need to be triggered. This can lead to increased shutdown time of the reactor, which means the costs of the maintenance would increase dramatically. Much like other large power-generating installations, the cost of downtime for EU-DEMO is expected to be in the millions of euros per day [4]. Since one of the goals of the EU-DEMO is to prove the cost-effectiveness of Fusion, this means that the sensor systems used for RM must be robust to the failure of any one device or sensor which could delay the completion of the maintenance tasks.

In industry, the traditional mobile robots, mainly AGVs, have their own sensors installed on board [3]. In addition, the principle of operation is mainly based on odometry measured by its internal sensors and one external sensing technology (e.g. sonars, LIDAR) [5]. However, the scenario conditions found in industry, mainly assembly and storage warehouses, where AGVs are used, are different from nuclear facilities. In addition, in case of failure, the failed AGV is simply moved aside, replaced by an operational one and set to wait for a technician to be repaired. This approach cannot be assumed in a nuclear facility, especially when transporting heavy activated loads.

In nuclear facilities/scenarios, the radiation effect is by far the most important issue for the common technologies of robotics available for industry, even during a machine shutdown. In ITER the rates will be in the order of hundreds of Gy/hour [6], and in DEMO they will be a minimum of 1 kGy/hour in-vessel [7]. Sensors, the most sensible parts of the mobile platforms, are commonly installed onboard and thus exposed to the radiation in the environment and especially that of the transported load (sensors are close to it). Therefore, in order to mitigate the risk of failure, the most appropriate sensing technologies need to be selected and combined. These should operate on different principles in order to provide maximum redundancy and minimising the risk of simultaneous breakdowns. [8] presents well-known and mature navigation technologies used by AGVs in industry: with a physical path (e.g., wire/inductive guidance, optical line guidance and magnetic tape guidance) and with a virtual path (e.g., laser based, motion capture, inertial, magnetic-gyro) to be followed by the AGV during the operations of transportation. For maximum flexibility and reliability, on-board situational awareness sensors should be used. Radiation shielding is impractical due to the weight penalty it would impose on a mobile robot, so radiation tolerant sensor systems must be developed. Even these radiation-hardened sensors will eventually fail, so combining the data from multiple different technologies is recommended to ensure redundancy.

Sensing technologies is a changing world, mature sensors are getting more sophisticated and new technologies are arising. In particular the sensing technologies related to virtual paths, where few or no intervention is required in the scenario and can be used beyond the path following.

This work is mainly focused on comparing three different technologies with particular interest in the robotics field at the moment and with potential advantages for nuclear facilities. These technologies are based on 1) image and depth cameras, 2) LIDAR systems and 3) mmWave radars. Other groups have investigated and compared the performance of remote sensors - for a general overview, see [9]. For a review focused on industrial applications of these technologies, see [10]. It is a common approach to combine more than one remote sensing technology (see [11] for a LIDAR-depth camera example and [12] for LIDAR-radar), but to our knowledge no other paper has evaluated the use of all three of these technologies in a nuclear remote maintenance context. In addition, we have the focus of making the results intuitively understandable for Fusion researchers working outside Remote Maintenance.

The remainder of the paper is organized as follows. Section 2 presents the justification for why remote sensing is needed in Nuclear facilities. Section 3 provides explanations for how the sensing technologies in question work. Section 4 compares the performance and environmental sensitivity of the sensor technologies. Section 5 presents the comparison tests carried out for this paper. Finally, Section 6 concludes the paper with relevant remarks and areas of interest for further work.

2. Remote sensing needs in nuclear facilities

Remote sensing is concerned with the perception of the environment surrounding by sensors installed on the mobile platform (onboard sensors) or installed on the building (offboard sensors). The most commonly used approach is based on onboard sensors, such as in industries, where the AGV carry the required internal (to measure internal signals) and external sensors (to measure environment values). [8]. In some configurations, additional elements can be installed on the scenario to improve the performance of the onboard sensors. These elements are normally passive, such as beacons or reflective markers used for optical devices, as detailed later in Section 3. No matter where the sensors are installed, these devices perform acquisitions of physical quantities present in the scenario, and translate them into electrical signals that are sent to a central processing unit (CPU). The CPU can be installed on the mobile platform or in a remote control room, outside of the operation area where human being are not allowed, often referred to as the *Red Zone*.

The electrical signals collected by the sensors comprises the remote sensing of the surrounding scenario, i.e., the sensor data, that can be used for different purposes. The sensor data is characterized by the type of information acquired, accuracy, precision, resolution, frequency of acquisition, time of response, etc. Consequently, each sensor must be allocated for specific tasks according to its specifications.

Once the sensor data reaches the CPU, it is able to i) compute the data to take decisions in real time, and ii) send the data with or without pre-processing such as compression, to a remote control room for different purposes. This configuration is similar to industrial facilities, however the remote sensing can be extended to outboard sensors, i.e., sensors installed on the building [13] which send the data directly to a control room. The data acquired by different types of onboard and offboard sensors must satisfy the following sensing needs in particular for mobile platforms:

- run in autonomous configuration by means of an on-board control system under monitoring of the supervisory control system;
- follow predefined computed trajectories and avoid collision with other equipment to prevent damage [14];
- localize in the scenario, with a pose (position and orientation) estimation, identifying the level of confidence; [13] [15]
- alignment and feedback during docking;
- provide information required to feed a Digital Twin system to simulate all the RM system to optimize logistics procedures and mitigate the risks of failure; and
- support for remote and rescue operation, when and where necessary.

The sensing technologies addressed to satisfy the needs presented above, in particular the offboard sensors, can also be envisaged to other purposes beyond the mobile platform. For instance, to supervise static robotic manipulators, to perform inspections in the scenario and to perform surveillance of unexpected issues, such as leakage detection.

3. Three key sensing technologies

In this section, we introduce three key types of sensing technologies which are often used for mobile robot navigation in the robotics field at the moment. Each technology is illustrated by a Commercial off-the-shelf (COTS) sensor, as depicted in Figure 2c. The key types of sensing technologies are:

1. **Colour-depth/RGB-D cameras** such as the Microsoft Kinect, Intel RealSense (Figure 2a) and similar devices
2. **LIDAR** (Light Detection And Ranging) such as the VLP-16 (Figure 2b)
3. **Millimetre-Wave RADAR** such as the TI AWR 1443 (Figure 2c)

3.1. Colour-Depth Cameras

Colour-depth cameras, also referred to as *RGB-D cameras*, are well established for use in mobile robotics applications. They are made up of two main components: 1) a standard digital camera capturing RGB-data and 2) a projector-sensor system capturing depth data. This depth system can function in different ways, one of which is projecting a grid of structured light in a non-visible spectrum onto a scene, and then interpret the distortions of this grid/pattern to determine the distance to - and shape of - any object which is in front of it. This is the reason RGB-D cameras are sometimes referred to as *Structured Light Cameras*. This data is then combined with the feed from a standard digital camera to produce a coloured 3D point cloud. The technology is affordable, lightweight, requires low power and it is a quite mature technology. However, one major drawback with this technology is the short range of the depth sensor – it relies on a light projection and the effective range is between 1 and 8 meters, typically no more than 10 m.

For comprehensive reviews of the use of these sensors in robotics, see, for instance, [16]. In addition, a first study of applying colour-depth cameras was performed in 2013 about the localization of Cask and Plug Remote Handling System in ITER using multiple video cameras for motion Capture [14].

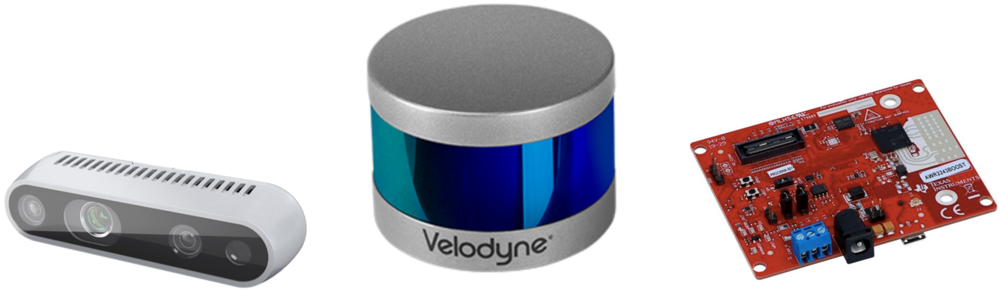

(a) RGB-D sensor: Intel RealSense d435 (b) LIDAR: Velodyne VLP-16 Puck (c) mmWave radar: Texas Instruments AWR1443

Figure 2: Example sensors of each type being compared; also the sensors used in Section 5 for comparison.

3.2. LIDAR

LIDAR sensors work by utilising one or more laser distance measurement sensor(s) to bounce a laser beam of surrounding objects to rapidly scan a scene, sometimes in a focused area and sometimes by scanning, i.e., rotating the laser emitter and receiver around an interval angle (e.g. full 360 degrees) and varying the angle of the internal distance measurement sensor. LIDAR sensing is very mature technology (since the late 80s) and are often used in the automotive and industrial sectors to measure distances and provide situational awareness.

Several approaches have been developed considering the LIDAR sensors as onboard sensors. However, motivated by the acute characteristics of transported loads, we have investigated the use of laser range finders as off-board sensors for mobile robotic vehicle localization in ITER ex-vessel [13] and [15]. In addition, we have also tested LIDAR scanners for use as on-board sensors inside the Joint European Torus tokamak during its 2016-17 shutdown (see [17] and [18]). This work combined sequential 2D LIDAR scans with a digital RGB camera data to create a coloured point cloud.

3.3. Millimetre-Wave RADAR

The millimetre-Wave RADAR works similarly to more traditional RADAR technology in that electromagnetic signals are sent out from an antenna and bounced off of obstacles, returning an echo which is detected. This echo is timed, and this provides a measurement of distance. More recently, this technology has been miniaturised to the point where the whole RADAR fits on a small circuit board with integrated send and receive antennas, and the way these signals are generated is based on a frequency modulation continuous wave (FMCW) principle where a *chirp* with rapidly changing frequency is emitted by the radar. Like LIDAR, it has pulsed time-of-flight and continuous-wave variants, including FMCW. This measures the frequencies returning from a continuous frequency-modulated beam rather than a pulse. The emitted signal is modulated with a sinusoidal or square wave with a frequency in the range of 10-100Mhz.

Sensors based on millimetre-Wave RADAR have become increasingly compact and well-performing during the last few years, and are increasingly used for obstacle detection and avoidance in the fields of mobile robotics and automotive sensing due to their small footprint, low weight, lack of moving parts, and the fact that the radar signals are not typically affected by rain, snow or smoke. For an example of a dataset including radar data collected and made available for autonomous car research, see [19]. For an evaluation of the potential of creating navigation maps using mmWave radar, see [20]. A recent development in the field is *milliMap*, a single-chip mmWave radar based indoor mapping system targeted towards low-visibility environments to assist in emergency response [12]. This utilises the AWR1443 sensor in order to create a map of an indoor scenario with smoke (same sensor which we use in our own experiments, see Section 5). For an illustration of the types of data returned by these sensors, cf. Figure 3.

In summary, the three sensing technologies presented above have potential to be used in nuclear facilities. However, the way of working, as well as the type of collected by these sensors are considerately different.

The next section compares these sensing technologies in detail.

4. Comparisons between sensing technologies

In this section, we highlight the differences between the technologies introduced in Section 3 as well as the effects this has on their performance and durability.

		Cost ($)	Weight (kg)	Power (W)	Scan Points
	Lidar (VLP-16)	8,000	0.83	8	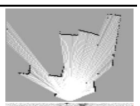
	Mechnical Radar (CTS-350)	Custo-mized Only	6	24	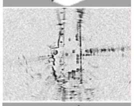
	Single-chip Radar (AWR1443)	299	<0.03	2	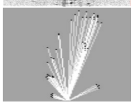

Figure 3: Illustration of data provided by two different types of RADAR sensor as well as a LIDAR. Image from [12].

The sensing technologies are necessary in the following three scenarios of Nuclear Fusion facilities:

1. In-Vessel (high rad), inspection by generating 3D reconstructions (ambitious, long-term)
2. Ex-vessel (lower rad), Mobile robotics to help when navigating around, transporting tools, components, radioactive materials etc.
3. Repair/Maintenance Facility etc., this will be a lot like the ex-vessel and like Decommissioning

At present, none of these sensing technologies would survive a large radiation dose. Therefore, the comparison is mainly focused on ex-vessel scenarios, where the lower levels of radiation are expected. However, work to create radiation tolerant versions are ongoing, and by investigating the complimentary nature of these technologies we can fully understand which technology is most appropriate for what application once more rugged versions become available, and how these technologies can best compliment each other. Besides radiation levels, nuclear scenarios include additional constraints not common in industries, such as residual magnetic fields, dust (especially contaminated dust), bad lighting conditions, as well as the restriction that human beings are not able to enter the area in most of the cases, even in situation of failure. The individual specification of each type of technology is important to evaluate its applicability in nuclear scenario.

Table 1 summarizes the main criteria of comparison used to evaluate the sensing technologies:

- type of information gathered in the operation scenario;
- maximum range expected in conditions of nuclear galleries;
- data density or equivalent to resolution;

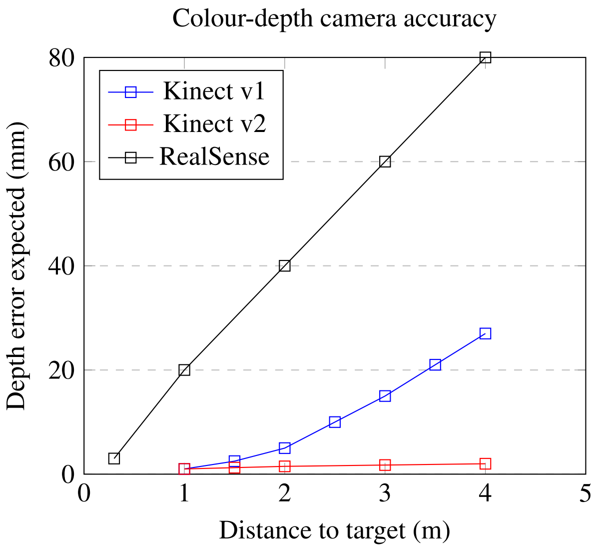

Figure 4: Chart showing accuracy at different distances for Kinect version 1 and 2 [21]. Data for Intel RealSense extrapolated from official datasheet [22].

- post-processing of data required for use;
- the potential environmental resistance of the sensor (gamma radiation);
- severity to dust expected in nuclear scenarios;
- field of view;
- data rate or frequency;
- measurement per second.

In the next subsection we review the expected accuracy achievable in realistic scenarios with these three types of sensors, as well as the progress in making these three types of sensor capable of operating in Fusion facilities and discuss possible mitigation.

4.1. Colour-Depth Cameras

The Microsoft Kinect v1, released in 2011, helped to kick-start the usage of Colour-Depth Cameras for mobile robotics. The Kinect version 2 was released in 2014 and uses a slightly different technology for its depth perception. As such, many papers have investigated the accuracy of one or both of these sensors, for example [21]. The range of the Version 1 is given as 0.7m - 6.0m, and the range of the Version 2 is 0,8m - 4.2m. In [23], the authors examine the accuracy over the full range of both sensors. This data can be seen in Figure 4. Other colour-depth cameras appeared in the market, such as the Structure Sensor 3D [24]. Work was

Technology type	RGB-D/Depth sensor	LIDAR	RADAR
Sensor example	Intel RealSense	Velodyne VLP-16	TI AWR 1443 mmWave
Type of information	Light collection and projected structured light	Laser signal bounced off target and measured	Millimetre-Wave radio signals emitted and received
Range	Low	High	Medium
Data density	High (colour and depth data)	Medium	Low
Required Post-processing	Medium	High	Low
Progress in radiation hardening	Medium (RGB)	Medium	Low
Sensitivity to dust	High	Medium	Low
Field of view	70°x 60°	360°x 30°	90°x 45°
Data rate	Color: 1920 x 1080 pixels, up to 60 fps Depth: 720 x 720 pixels, up to 30 fps	200MB/min point clouds	several KB/min (adjustable number of strongest returns)
Sampling	30 FPS	5-20 Hz	6M-12M samples per second

Table 1: Comparison of sensor features.

done combining this camera with a radiological sensor and both installed on a COTS UAV for 3D reconstruction of a scenario and radiological hotspots detection and localization, [25]. The initial version of this sensor only included depth and greyscale images. The most recent version already included colour. Probably, the most popular colour-depth camera at the moment is the Intel RealSense, which has a range up to 10m, an error rate of 2% of distance (according to the manufacturer), and provides high resolution coloured images. The accuracy of the most used cameras (Kinect versions 1 and 2 and RealSense) is plotted in Figure 4.

Since colour-depth cameras are effectively made up of two separate sensors which are combined, both parts (RGB and Depth) have to be radiation hardened. Work carried out for ITER Remote Maintenance has suggested digital CMOS cameras could be developed with several MGy of lifetime tolerance [26], demonstrating the feasibility of designing a CMOS RGB camera-on-a-chip with a lifetime tolerance above 6 MGy. This leaves the Depth sensor portion and the on-board processing CPU of the sensor needing radiation hardening. These components remains the biggest challenge for utilising this type of sensor in a nuclear environment.

4.2. LIDAR

LIDAR sensors operate over a large range, and unlike Colour-Depth cameras, the distance error does not vary appreciably over this range. For example, the accuracy of the VLP-16 has been reported to be +-2 cm over most of its 100m range [9] . Indeed, onboard LIDAR systems has been demonstrated to be capable of localising a mobile robot in oil-gas environment, with 1- 2cm accuracy [27]. In another piece of work, a co-located LIDAR and Camera both implemented in the same hardware achieved a resolution of 3.5cm over a 5m range when being used for AGV navigation [28].

Steps are also being taken to improve the tolerance of LIDAR scanners. LIDAR scanner components such as Time-to-Digital converters have been created with a radiation tolerance of 5 MGy [29], and Time-to-Digital converters which can be used for LIDAR receivers have been created with 1 MGy radiation tolerance [30]. While the achievable radiation tolerance levels for a full LIDAR system are not yet known, this raises the real possibility that such sensors could become available for high-radiation environments. Commercial off the shelf LIDAR sensors have also been radiation tested, and in one test the STMicroelectronics VL53L0X LIDAR mudule was tested to 5.8 kGy without issue, once the on-board DC voltage regulator was replaced with an external supply [31].

4.3. mmWave Radar

Though FMCW radars are very compact and versatile, extracting useful location and velocity data from the raw signals requires a fair bit of processing. This is normally done on-board the device itself and so does not need to trouble the user, but this does limit the performance compared to other types of radar [32].

Radar sensors have other problems not faced by lasers or cameras. The beams are less focused, allowing for coverage of a wide area in a single pulse, but making spatial accuracy poor. Systems with multiple antennas, or a more focused steered beam, can help mitigate this. Regarding depth accuracy, phase evaluation algorithms have been developed which enable a range accuracy of within about 5 micrometers over a measurement range of at least 0.035 to 2 m [33] [34] This shows the achievable accuracy in a laboratory setting and the promise of the technology in theory.

In real-world settings using portable devices, the accuracy is much lower, and there is a limit on how well different targets can be distinguished from each other. [35] found a minimum distinguishable range difference of 0.3m, below which two targets could not be separated and appeared as a single radar "peak".

In summary, mmWave radar accuracy performance can be difficult to quantify. On one hand, extremely impressive performance using a custom 80 MHz radar has been achieved in the lab but on the other, real-world performance is still a challenge.

The sensing element on the radar (antenna) is inherently rad-hard since it is just a piece of metal, though the on-board processing required is a hindrance in terms of making the sensor work in a high-radiation environment. One option would be to place the device in a shielded box with only the antenna on the outside if this box - this is a solution which the radar is much better suited for than the other sensors evaluated here.

4.4. Combining sensors data

The technologies described in Section 3 all provide reasonably reliable distance measurements in indoor or industrial environments. However, the way the data is collected and processed is very different, leading to a range of different strengths and weaknesses for each sensor. This means that often, combining two or more differing types of sensor can produce a more accurate or otherwise robust sensor value than only using one single sensor would allow.

Combining the output from several complimentary sensors is certainly nothing new. There is a range of publications available detailing the efforts made by other researches in combining these sensor technologies, both with each other and occasionally with other types of sensor. For example, [9] lists and compares performance of different LIDAR scanners and colour-depth cameras based on Time-of-Flight methods. [11] combined LIDAR and RGB-D data to enable navigation around uneven indoor environments. [36] combined radar odometry as well as Visual Odometry, and found that radar performs better on flat featureless areas such as well, whereas visual sensors perform better in cluttered environments. [37] found that mapping using both LIDAR and RGB-D point clouds combines the benefits of LIDAR when it comes to measurement accuracy and RGB-D for feature extraction. [38] combines a mm-wave portable scanner concept with a depth camera for people scanning. They are merged to show both the external layer of the object (global point cloud) and the second one related to inner layers (global reflectivity).

Since all sensors have benefits and drawbacks, it is likely the best solution will come from deploying a range of different sensors based on different principles in order to minimise the effect of any one technological failure or issue causing catastrophic results.

5. Experiments

In order to further explain and highlight the differences between the 3 technologies which this paper focuses on, we designed an experiment which combined all three on a single platform. In this, our goal was not to achieve an especially high level of accuracy, but to produce a basic demonstration of what can be done with currently available off-the-shelf sensors which can be obtained by most researchers, and to present the results in a way which allows non-specialists to get an intuitive understanding of the differences in the data which each of these types of sensor produces.

We selected the following sensors, since they are commonly used for research and reasonably priced compared to other sensors of their type:

- **Colour-Depth Camera:** Intel RealSense d435
- **LIDAR:** Velodyne VLP-16
- **mmWave radar:** TI mmWave Demo AWR 1443 BOOST

For photographs of these sensors, cf. Figure 2.

5.1. Experimental Setup

In Figure 5, one can see the setup of the three sensors. All the sensors were secured on an aluminum case, where the power source and CPU are enclosed. This case was designed to be robust enough to secure heavy sensors such as the LIDAR, even on rough terrain.

During the experiment, the setup was carried by a person at waist height (~1m), but the apparatus can also be transported by ground vehicles or even drones. The colour-depth camera and the radar are facing forward and as such the person carrying the case does not compromise the collected samples. On the other hand, the

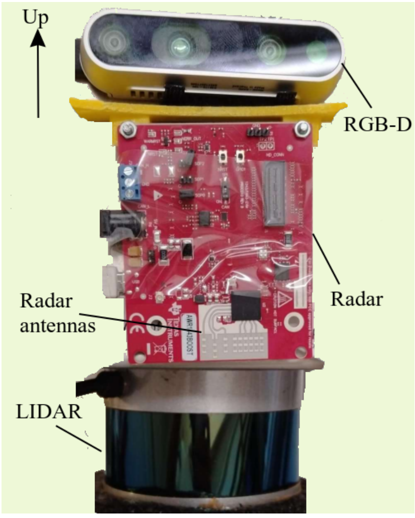

Figure 5: Three-sensor setup used to perform the tests.

LIDAR collects information all around 360º, therefore all points at short range (<1m) were removed.

The LIDAR was powered directly by a 3S Lipo battery (12V), while the radar was powered by a 12DC/5DC power converter. The CPU in use was a Nvidia Jetson Nano, powered by the same DC/DC unit. The colour-depth camera was powered by USB from the Nano.

The Jetson runs Ubuntu 18.04 and had installed ROS Melodic. Offical ROS Packages for all three sensors were installed, and nodes published point clouds periodically to individual topics. All samples were collected into ROS Bag files, and later analyzed, transformed and visualized using the PCL 1.8 library. The coding language used was C++.

5.2. Methodology

Since the LIDAR is the *de facto* standard for 3D reconstruction and it is known to provide the greatest precision when compared to the other technologies, we considered the LIDAR to be our ground-truth.

Once the data had been collected, the second step was to reconstruct the 3D scenario using LIDAR data and a SLAM algorithm (ALOAM [39]). We have tested other methods in the past, such as LOAM and HDL-SLAM , but in general ALOAM is sufficient for the task of generating a meaningful 3D scenario, namely a thin floor plane and flat walls. Besides registering LIDAR frames into a fixed referential, ALOAM also computes the estimated path (pose and position).

Later, both radar and RGB-D frames were transformed (rotations and translation) according to their pose and position relative to the LIDAR. Finally, these point clouds were registered into the world fixed referential using the ALOAM generated path, and at the end saved into PCD files.

5.3. Experimental Results

Multiple trials were performed along the same corridor, all with very similar results. We show the point clouds, from one of the trials inside a university campus building corridor. This is a representative environment since large corridors are a common feature in most nuclear installations, including nuclear fusion installations [14]. This location encompasses multiple metal objects namely decorative airplane engines, and is surrounded by metal doors and windows. Other objects such as wood benches are also present. These features can be seen in Figure 6. The top photograph was taken close by the assumed origin of the (world) fixed referential.

Figure 6: Indoor test scenario. Top image is facing the direction of movement during the trial. Bottom image, shows the opposite view.

The output from each sensor provides a very different set of information about the scene. As a matter of reference, in this particular trial we collected data for 49s, overall producing 1GB of compressed data (ROS lz4 compression). While the LIDAR and RGB-D camera generated around 1.5 million points, the radar output produced only around 18k points. Overall, RGB-D data

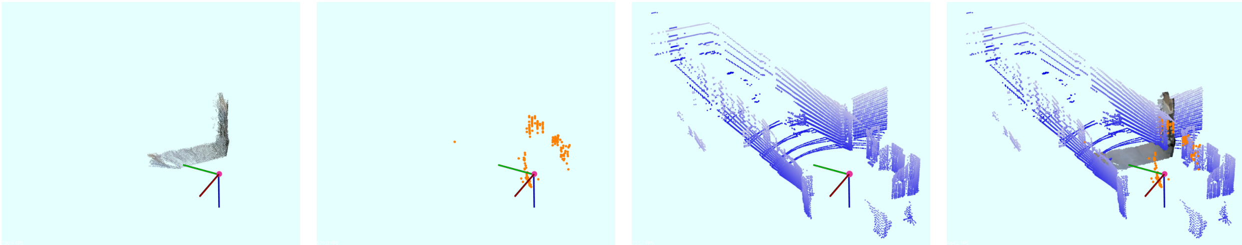

(a) RGB-D sensor: Intel RealSense (b) mmWave radar: TI AWR 1443 (c) LIDAR: Velodyne VLP-16 Puck (d) All three sensors

Figure 7: A single *frame* from each one of the sensors.

utilizes more space than the LIDAR since RGB color is also stored.

In Figure 7, one can compare the major differences of the datasets of a single *frame*, where we can define a frame as a single point cloud we collect at a given time. LIDAR has a great range and detail; it is able to detect the end of the corridor event at the start. Radar produces only data very close to the sensor and hard to comprehend without the LIDAR as a reference. RGB-D generates a detailed view of the near by area, despite the limited field of view, barely reaching both walls at the same time.

When considering all data collected while moving the sensing platform along the corridor, we obtain a better picture of the sensors performance. In Figure 8, on can see an isometric, upper view of the corridor and in Figure 9 we can see the same data from a top-down view. The pink line represents the motion along the corridor, starting at the top-right corner and ending at the bottom-left corner of the view. It is present in all views for orientation of the reader. The point clouds from LIDAR and RGB-D provide plenty of 3D detail. It is clear that the LIDAR provides superior performance regarding precision and better coverage (higher FoV). RGB-D is able to grasp the true colors of the environment as well as a good 3D structure, but only provides data at a very short range. The radar dataset is noisier, but nevertheless able to detect major features such as the floor directly in front to the sensor, the walls and windows metal frames, and lastly the two big airplane engines on site. In addition, the fact that the radar dataset is very sparse can provide an advantage in that less processing is required to handle the data.

In Figure 10, one can see in detail one of the airplane engines, namely the one shown in the top photograph of Figure 6. It is clear that all sensors can *see* it.

Note that while the LIDAR has 360°FoV, the other sensors had to be facing such features to guarantee they were not missed. That is the reason why the bottom-left view of Figure 9a and Figure 9c are missing information. The LIDAR also missed some floor in the beginning and at the end of the path, due to its vertical FoV limitations (cf.Figure 9b).

6. Conclusion

The challenge of how to provide adequate remote sensing in nuclear environments such as Fusion remote maintenance, decommissioning or other nuclear applications will not be solved by a single technology. For reasons of redundancy and robustness to unexpected errors, it is desirable to utilise several sensors based on differing sensing modalities and implementation technologies. This will ensure that no single technological weakness or situation will cause the whole system to fail.

Our experiments highlight the varying amounts of data provided from different sensors in order to extract required information for a task such as obstacle avoidance: the radar information displayed in Figure 9c can be used to avoid obstacles with a much smaller number of points being processed by the system. However, the low data density provides a less comprehensive view of the environment, limiting the capabilities to produce a robust map and contextual information such as clear object shapes. Color/RGB-D sensors also provides high data density and high levels of environmental awareness, but are hampered by the requirement for consistent lighting levels for quality RGB images as well as the short range of their depth camera elements. This highlights the value of utilising multiple sensors for remote sensing tasks.

The results from our experiments combining LIDAR and radar data can be seen in Figure 9d. This is a clear example of the different data densities highlighted in Table 1.

It was also our goal to provide an intuitive understanding of the differences (including pros and con) between the types of data provided by these different sensor technologies to researchers in the Fusion field who may not be knowledgeable about robotics. We believe the sensor data figures provided accomplishes this task, since they provide a clear indication as to how a particular sensor *sees* its surroundings.

The most sensible part of each one of the three technologies presented herein, are exposed to radiation. Therefore, none of these technologies would survive a large radiation dose. The LIDAR is probably the best candidate technology to protect the sensor by a set of mirrors. The same approach can be used for the cameras, but probably only for the RGB part and not for the depth, since the mirror glass affects the performance of light project and, hence, the estimation of distances. The radar could have its antenna placed outside of a shielded box with the processing part inside, but shielding would only add a limited amount of lifetime unless prohibitively thick and heavy shielding is used. In summary, the expected time life of these technologies are similar. Combining different sensors working in parallel, rather than improve the quality of the data, provides the ability to understand when one of the sensors started to malfunctioning. A recovery operation can be triggered and a rescue operation is avoided, which is an important benefit in terms of costs and interruption during a maintenance of a power reactor.

Future work will include further testing of different combinations of the sensor technologies presented here in differing scenarios in order to better characterise their performance. Could also look at the different types of robot expected in fusion ex-vessel and which sensor fits which type of robot.

7. Acknowledgements

This work has been carried out within the framework of the EUROfusion Consortium and has received funding from the Euratom research and training programme 2014-2018 and 2019-2020 under grant agreement No 633053. IST activities also received financial support from "Fundação para a Ciência e Tecnologia" through projects UIDB/50010/2020 and UIDP/50010/2020. The views and opinions expressed herein do not necessarily reflect those of the European Commission.

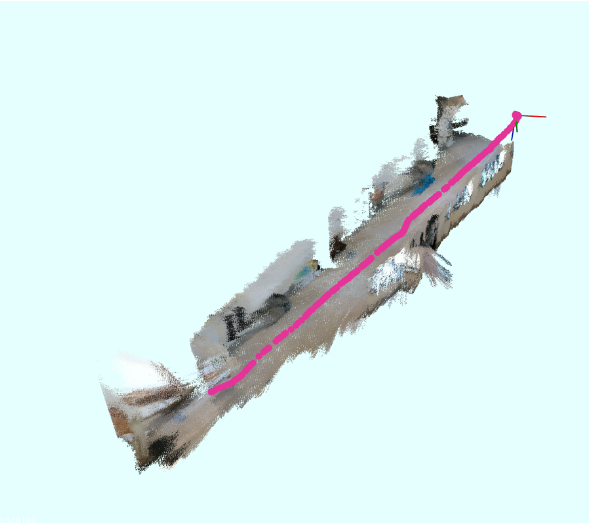

(a) RGB-D sensor: Intel RealSense

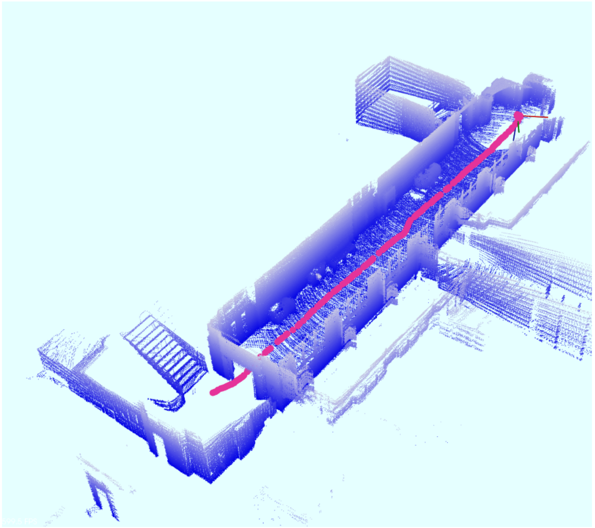

(b) LIDAR: Velodyne VLP-16 Puck

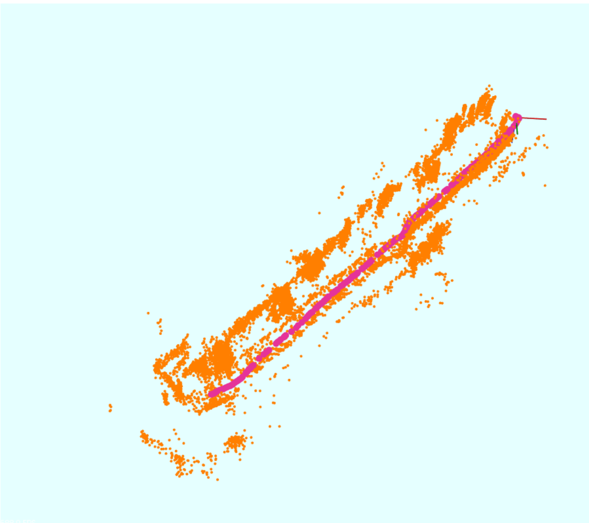

(c) mmWave radar: Texas Instruments AWR 1443

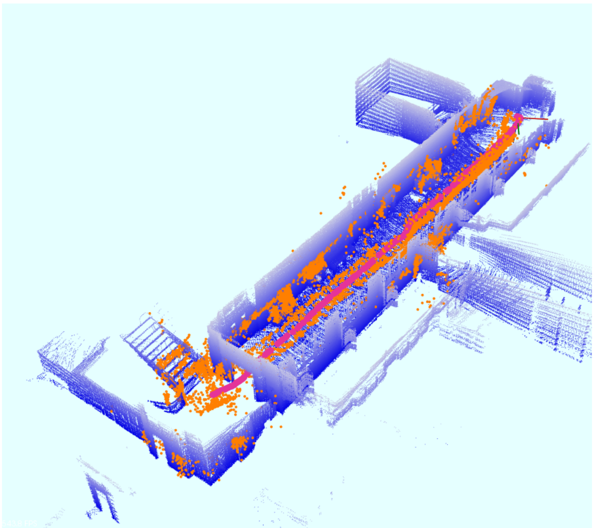

(d) All three sensors

Figure 8: Isometric like views of the data of each sensor individually – a),b) and c), and all data merged – d).

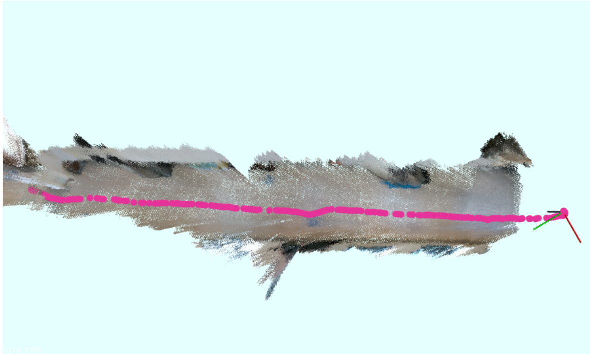

(a) RGB-D sensor: Intel RealSense

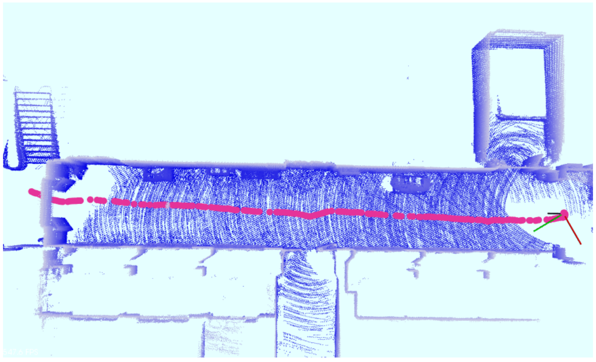

(b) LIDAR: Velodyne VLP-16 Puck

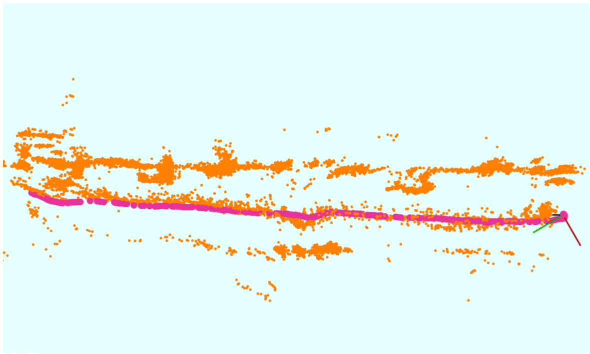

(c) mmWave radar: TI AWR1443

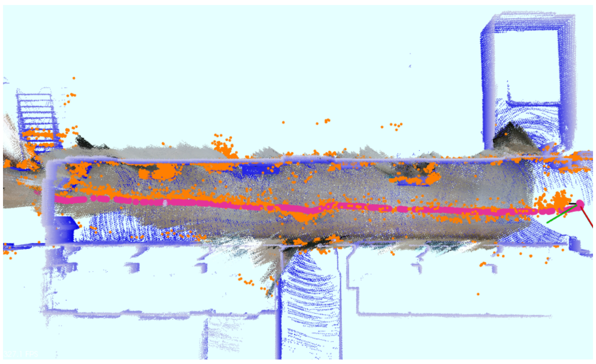

(d) All three sensors

Figure 9: Topview of the corridor, selecting different sensor datasets.

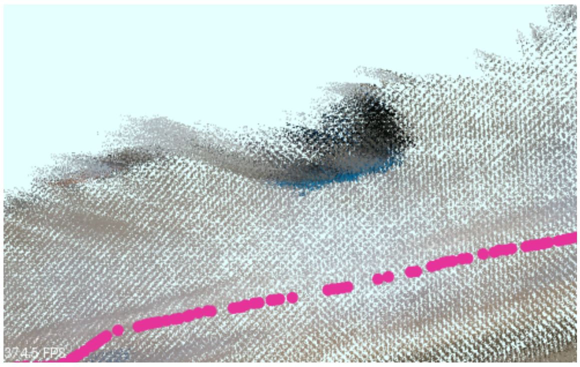

(a) RGB-D sensor: Intel RealSense

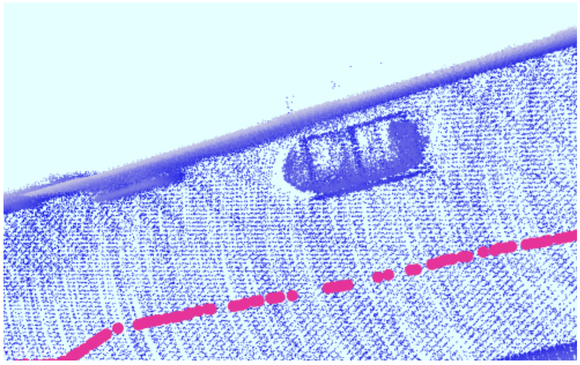

(b) LIDAR: Velodyne VLP-16 Puck

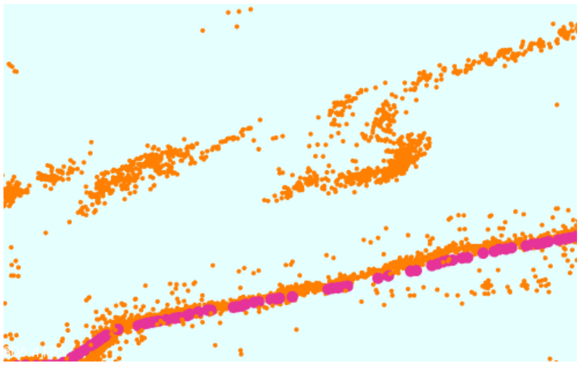

(c) mmWave radar: TI AWR1443

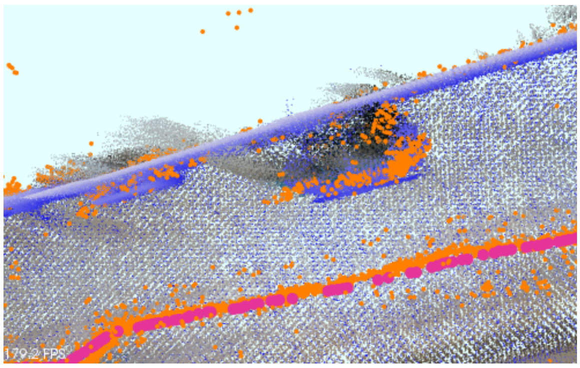

(d) All three sensors

Figure 10: Detail of a metal engine on the corridor, selecting different sensor datasets

References

[1] O. Crofts, A. Loving, D. Iglesias, M. Coleman, M. Siuko, M. Mittwollen, V. Queral, A. Vale, E. Villedieu, Overview of progress on the European DEMO remote maintenance strategy 109-111 (2016) 1392–1398. doi:10.1016/j.fusengdes.2015.12.013.

[2] C. G. Gutiérrez, C. Damiani, M. Irving, J. P. Friconneau, A. Tesini, I. Ribeiro, A. Vale, ITER Transfer Cask System: Status of design, issues and future developments 85 (10) (2010) 2295–2299. doi:10.1016/j.fusengdes.2010.09.010.

[3] A. Vale, Assessment of ex-vessel transportation in remote maintenance systems of DEMO 98-99 (2015) 1660–1663. doi:10.1016/j.fusengdes.2015.06.158.

[4] N. Petkov, H. Wu, R. Powell, Cost-benefit analysis of condition monitoring on DEMO remote maintenance system 160 (2020) 112022. doi:10.1016/j.fusengdes.2020.112022.

[5] R. Siegwart, I. R. Nourbakhsh, D. Scaramuzza, Introduction to Autonomous Mobile Robots, second edition Edition, The MIT Press, 2011-02-18.

[6] C. Damiani, J. Palmer, N. Takeda, C. Annino, S. Balagué, P. Bates, S. Bernal, J. Cornellá, G. Dubus, S. Esqué, C. Gonzalez, T. Ilkei, M. Lewczanin, D. Locke, L. Mont, B. Perrier, A. Puiu, E. Ruiz, R. Shuff, N. Van De Ven, C. Van Hille, M. Van Uffelen, C. H. Choi, J. P. Friconneau, D. Hamilton, J. P. Martin, S. Murakami, R. Reichle, J. S. Cuevas, T. Maruyama, Y. Noguchi, M. Saito, Overview of the ITER remote maintenance design and of the development activities in Europe 136 (2018) 1117–1124. doi:10.1016/j.fusengdes.2018.04.085.

[7] C. Bachmann, S. Ciattaglia, F. Cismondi, T. Eade, G. Federici, U. Fischer, T. Franke, C. Gliss, F. Hernandez, J. Keep, M. Loughlin, F. Maviglia, F. Moro, J. Morris, P. Pereslavtsev, N. Taylor, Z. Vizvary, R. Wenninger, Overview over DEMO design integration challenges and their impact on component design concepts (2018). doi:10.1016/j.fusengdes.2017.12.040.

[8] A. Vale, R. Ventura, P. Lopes, I. Ribeiro, Assessment of navigation technologies for automated guided vehicle in nuclear fusion facilities 97 (2017) 153–170. doi:10.1016/j.robot.2017.08.006.

[9] R. Horaud, M. Hansard, G. Evangelidis, C. Ménier, An overview of depth cameras and range scanners based on time-of-flight technologies 27 (7) (2016) 1005–1020. doi:10.1007/s00138-016-0784-4.

[10] L. Pérez, Rodríguez, N. Rodríguez, R. Usamentiaga, D. F. García, Robot Guidance Using Machine Vision Techniques in Industrial Environments: A Comparative Review 16 (3) (2016) 335. doi:10.3390/s16030335.

[11] C. Wang, J. Wang, C. Li, D. Ho, J. Cheng, T. Yan, L. Meng, M. Q.-H. Meng, Safe and Robust Mobile Robot Navigation in Uneven Indoor Environments 19 (13) (2019) 2993. doi:10.3390/s19132993.

[12] C. X. Lu, S. Rosa, P. Zhao, B. Wang, C. Chen, J. A. Stankovic, N. Trigoni, A. Markham, See Through Smoke: Robust Indoor Mapping with Low-cost mmWave Radar (2020). arXiv:1911.00398.

[13] J. Ferreira, A. Vale, R. Ventura, Vehicle localization system using offboard range sensor network 46 (10) (2013) 102–107. doi:10.3182/20130626-3-AU-2035.00032.

[14] J. Ferreira, A. Vale, I. Ribeiro, Localization of cask and plug remote handling system in ITER using multiple video cameras 88 (9) (2013) 1992–1996. doi:10.1016/j.fusengdes.2012.10.008.

[15] T. Sousa, A. Vale, R. Ventura, Calibration of Laser Range Finders for Mobile Robot Localization in ITER, 2015, pp. 541–549.

[16] G. Alenyà, S. Foix, C. Torras, ToF cameras for active vision in robotics 218 (2014) 10–22. doi:10.1016/j.sna.2014.07.014.

[17] E. T. Jonasson, J. Boeuf, S. Kyberd, R. Skilton, G. Burroughes, P. Amayo, S. Collins, Reconstructing JET using LIDAR-Vision fusion 146 (2019) 110952. doi:10.1016/j.fusengdes.2019.03.069.

[18] E. T. Jonasson, J. Boeuf, P. Murcutt, S. Kyberd, R. Skilton, Improved reconstruction of JET using LIDAR-Vision fusion 161 (2020) 112061. doi:10.1016/j.fusengdes.2020.112061.

[19] D. Barnes, M. Gadd, P. Murcutt, P. Newman, I. Posner, The Oxford Radar RobotCar Dataset: A Radar Extension to the Oxford RobotCar Dataset (2020). arXiv:1909.01300.

[20] B. Clarke, S. Worrall, G. Brooker, E. Nebot, Towards mapping of dynamic environments with FMCW radar, in: 2013 IEEE Intelligent Vehicles Symposium (IV), 2013-06, pp. 147–152. doi:10.1109/IVS.2013.6629462.

[21] H. Gonzalez-Jorge, P. Rodríguez-Gonzálvez, J. Martínez-Sánchez, D. González-Aguilera, P. Arias, M. Gesto, L. Díaz-Vilariño, Metrological comparison between Kinect I and Kinect II sensors 70 (2015) 21–26. doi:10.1016/j.measurement.2015.03.042.

[22] Intel RealSense D400 Series Data Sheet (2020).
URL https://www.intel.com/content/dam/support/us/en/documents/emerging-technologies/intel-realsense-technology/Intel-RealSense-D400-Series-Datasheet.pdf

[23] D. Pagliari, L. Pinto, Calibration of Kinect for Xbox One and Comparison between the Two Generations of Microsoft Sensors 15 (11) (2015) 27569–27589. doi:10.3390/s151127569.

[24] Structure by Occipital - Give Your iPad 3D Vision (2020).
URL https://structure.io/

[25] H. Carvalho, A. Vale, R. Marques, R. Ventura, Y. Brouwer, B. Gonçalves, Remote inspection with multi-copters, radiological sensors and SLAM techniques 170 (2018) 07014. doi:10.1051/epjconf/201817007014.
URL https://www.epj-conferences.org/articles/epjconf/abs/2018/05/epjconf_animma2018_07014/epjconf_animma2018_07014.html

[26] V. Goiffon, S. Rolando, F. Corbière, S. Rizzolo, A. Chabane, S. Girard, J. Baer, M. Estribeau, P. Magnan, P. Paillet, M. V. Uffelen, L. M. Casellas, R. Scott, M. Gaillardin, C. Marcandella, O. Marcelot, T. Allanche, Radiation Hardening of Digital Color CMOS Camera-on-a-Chip Building Blocks for Multi-MGy Total Ionizing Dose Environments 64 (1) (2017) 45–53. doi:10.1109/TNS.2016.2636566.

[27] P. Merriaux, Y. Dupuis, R. Boutteau, P. Vasseur, X. Savatier, Robust robot localization in a complex oil and gas industrial environment 35 (2) (2018) 213–230. doi:10.1002/rob.21735.

[28] S. Ito, S. Hiratsuka, M. Ohta, H. Matsubara, M. Ogawa, Small Imaging Depth LIDAR and DCNN-Based Localization for Automated Guided Vehicle 18 (1) (2018). arXiv:29320434, doi:10.3390/s18010177.

[29] Y. Cao, W. D. Cock, M. Steyaert, P. Leroux, Design and Assessment of a 6 ps-Resolution Time-to-Digital Converter With 5 MGy Gamma-Dose Tolerance for LIDAR Application 59 (4) (2012) 1382–1389. doi:10.1109/TNS.2012.2193598.

[30] TDC2201 – MAGICS (2020).
URL https://www.magics.tech/portfolio/rad-hard-asics/tdc2201/

[31] S. Chesnevskaya, C. Via, B. Utting, H. Hughes, S. Watts, Radiation testing of robotic systems – LiDAR as a case study - Abstract, 2019.

[32] Z. Peng, C. Li, Portable Microwave Radar Systems for Short-Range Localization and Life Tracking: A Review 19 (5) (2019) 1136. doi:10.3390/s19051136.

[33] L. Piotrowsky, T. Jaeschke, S. Kueppers, J. Siska, N. Pohl, Enabling High Accuracy Distance Measurements With FMCW Radar Sensors 67 (12) (2019) 5360–5371. doi:10.1109/TMTT.2019.2930504.

[34] M. Pauli, B. Göttel, S. Scherr, A. Bhutani, S. Ayhan, W. Winkler, T. Zwick, Miniaturized Millimeter-Wave Radar Sensor for High-Accuracy Applications 65 (5) (2017) 1707–1715. doi:10.1109/TMTT.2017.2677910.

[35] X. Gao, G. Xing, S. Roy, H. Liu, Experiments with mmWave Automotive Radar Test-bed (2019) 1–6arXiv:1912.12566, doi:10.1109/IEEECONF44664.2019.9048939.

[36] M. Mostafa, S. Zahran, A. Moussa, N. El-Sheimy, A. Sesay, Radar and Visual Odometry Integrated System Aided Navigation for UAVS in GNSS Denied Environment 18 (9) (2018) 2776. doi:10.3390/s18092776.

[37] C. M. Costa, H. M. Sobreira, A. J. Sousa, G. M. Veiga, Robust 3/6 DoF self-localization system with selective map update for mobile robot platforms 76 (2016) 113–140. doi:10.1016/j.robot.2015.09.030.

[38] J. Laviada, M. López-Portugués, A. Arboleya-Arboleya, F. Las-Heras, Multiview mm-Wave Imaging With Augmented Depth Camera Information 6 (2018) 16869–16877. doi:10.1109/ACCESS.2018.2816466.

[39] J. Zhang, S. Singh, Low-drift and real-time lidar odometry and mapping 41 (2) (2017) 401–416. doi:10.1007/s10514-016-9548-2.